Gas Processing Journal

Vol. 9, No. 2 2021, pp. 61-82
http://gpj.ui.ac.ir

Research Paper

Investigating a novel propulsion system for unmanned aerial vehicle equipped with PEM electrolyzer, PEM fuel cell, and hydrogen and oxygen storage tanks, using photovoltaic panel as renewable energy

Amirhamzeh Farajollahi[1*], Mohsen Rostami [2]

[1] Assistant Professor of aerospace engineering, Imam Ali University, Tehran, Iran
[2] Assistant Professor of aerospace engineering, Imam Ali University, Tehran, Iran

Received: 2022-03-12 Revised: 2022-04-01 Accepted: 2022-04-09

Abstract: Today, for enhancing the trend of energy demand in the world, the use of energy by the approach of maximizing the efficiency of energy systems is inevitable. On the other hand, the high growth rate of unmanned aerial vehicles (UAV), governments investment to develop the necessary infrastructures for the progress of this technology, the variety of applications, and the advantages, indicate its special role in the future. In the present study, an integrated system consisting of PEM electrolyzer, PEM fuel cell, photovoltaic panel, and hydrogen and oxygen storage tanks is developed as a UAV propulsion system so that it can provide the required power. The power required by the UAV was supplied by the PEM fuel cell of the system. The intended hydrogen and oxygen are provided through a hydrogen and oxygen storage tank. In this condition, the capacity of the tanks is known as the limiting factor during the UAV flight time. For more flight continuity, part of the consumable hydrogen and oxygen during the flight is regenerated by installing a photovoltaic panel, using solar renewable energy and also PEM electrolyzer. The hydrogen and oxygen generated by the electrolyzer is 49.04% of the PEM fuel cell consumption, indicating that the UAV flight continuity using the integrated structure of the present study can be increased up to approximately 1.5 times. Then, by performing a parametric study and changing the main parameters of the system, including current densities of PEM electrolyzer and PEM fuel cell, as well as temperature and solar radiation level, the integrated system is evaluated in different conditions and the results are reported. Finally, by examining various aspects of the present plan, including the weight conditions, the efficiency of the integrated system developed in the present study as a new propulsion system for UAVs with various purposes has been specified.

keywords: PEM fuel cell; Solar photovoltaic panel; PEM electrolyzer; Unmanned aerial vehicle

1. Introduction

All birds that can be remotely piloted for a specific mission are called drones. In the past, drones were used for operations such as reconnaissance and mapping, but today they have a much wider range of applications (Pan et al., 2019). Nowadays, with the increase in demand and construction of various types of unmanned aerial vehicles (UAV), naturally, the range of their use has become very wide, UAVs are used in the military(Gong & Verstraete, 2017), industrial (Boukoberine et al., 2019), artistic, agricultural (Adão et al., 2017)and recreational applications. The most important modern applications of UAVs are as follows.

- Aerial photography for journalism and film
- Fast transport and delivery
- Gathering information or providing supplies for crisis management
- Search and rescue operations
- Geographical mapping of land and inaccessible places
- Perform safety inspections
- Monitoring border control
- Tracking and forecasting storms and tornadoes
- Participate in military and defense operations
- Providing telecommunication services

A hydrogen storage tank is usually applied for supplying the required power of the drones so that the hydrogen is converted to power through a fuel cell polymer electrolyte membrane (PEM) by an electrochemical reaction and provides the required power of the drone (Gadalla & Zafar, 2016). Based on this type of propulsion engine, the volume of the hydrogen stored in the drone is considered a limiting criterion for its flight continuity. In fact, after the hydrogen runs out, drone refueling must be done(Bayrak et al.,

* Corresponding Author.
Authors' Email Address: [1] A. Farajollahi (a.farajollahi@sharif.edu), [2] M. Rostami (cpt.rostami@gmail.com)

http://dx.doi.org/10.22108/GPJ.2022.133040.1118

2020). In the present study, it has been proposed to supply hydrogen and oxygen required for fuel cells through an electrolyzer, so that in a closed water cycle, water first enters the electrolyzer as the working fluid of the cycle and is decomposed into hydrogen and oxygen molecules. Then, it enters the PEM fuel cell and generates power by performing an electrochemical reaction in the electrolytic substrate. Since the output of this reaction is water, this water re-enters the electrolyzer to form a closed cycle (without the additional water). Solar energy is also used to supply the required energy of the electrolyzer. A photovoltaic panel is provided for this purpose. By developing the present cycle, it is possible to achieve the continuous production of the energy required by the UAV. Since solar energy is the main source of this project, due to its uncertainty, a fuel storage tank can be considered as an auxiliary fuel to provide the required energy for the drone in the absence of the needed radiation.

Renewable energies come from natural resources that are constantly being replaced. Among them, solar and wind energies are the most available type of renewable energies. According to a report released by the International Energy Agency (IEA) on energy consumption, by 2050 solar power plants will meet about 45% of energy demand in various industries in the world (Ghorbani et al., 2021). Iran is located between 25 to 40 degrees north latitude and is located in a region that is among the highest in the world in terms of received solar energy. The average annual amount of solar radiation in Iran is estimated between 1800 to 2200 kWh per square meter per year, which is higher than the global average. In Iran, on average, more than 280 sunny days are reported annually, which is very significant. In recent years, the use of new energy sources has grown significantly due to the limitations and high cost of fossil fuels as well as environmental issues. To use solar energy, it must be converted into useful forms. Solar energy can be converted into three methods for different applications(Pandey).

A) Conversion of solar energy into chemical energy: Green plants convert solar energy into sugar and cellulose and convert it into chemical energy through the process of photosynthesis. All biomass contains chemically stored solar energy.

B) Conversion of solar energy to thermal energy: Solar heating devices convert solar energy into thermal energy that is used for drying, water heating, space heating, cooking, and water distillation. The cheapest and simplest uses of solar energy (for example, solar dryers and solar water heaters) raise the air or water temperature by 20 to 40 °C. When more energy and higher temperatures are required, Solar energy must be centrally transferred or stored, which greatly increases the cost and complexity of the required solar equipment.

C) Conversion of solar energy into electrical energy: Solar electrical devices convert solar energy into electrical energy. This can be used to directly supply power to electrical appliances or can be stored in storage devices (storage devices are often used at night or when solar radiation is not available).

Photovoltaic systems are used as units connected to the national grid or independently to supply electricity. The use of grid-independent photovoltaic systems can be very cost-effective and problem-solving in order to supply electricity to consumers who do not have access to the electricity distribution network for various reasons, including geographical conditions. Features of photovoltaic systems include their use on a small and large scale, the possibility of use in urban and rural areas, and the low time of their installation and launching, which makes them widely used among other methods of receiving solar energy. Direct conversion of solar energy into electricity is usually done by photovoltaic cells that use the photovoltaic effect. The photovoltaic effect is based on the interaction of photons with energies equal to or greater than the restricted band energy of the photovoltaic material. Photovoltaic cells convert solar energy into electricity without pollution or noise. Solar energy has a low density, so photovoltaic modules must have a large surface area to be able to produce enough energy(Muhammad Asif Hanif, 2022). Various studies have been presented on the different applications of photovoltaic systems. Mezzai et al. (Smith & Taylor, 2008)modeled and presented a hybrid photovoltaic/wind/fuel cell system. The proposed system is simulated using MATLAB Simulink software. In a study by Degobert et al. (Degobert et al., 2006), the combination of a photovoltaic system and a micro-turbine to generate power was investigated. This system has been studied in two independent states and connected to the local electricity network. The model is simulated and the results are compared with the analytical solution. Medrano et al.(Medrano et al., 2008) used a research center to conduct economic analysis and study the reduction of emissions of harmful gases to the environment. Modern energy systems such as solar photovoltaic panels, solar collectors, cogeneration internal combustion engine, and absorption chiller have been used in this center and the amount of energy consumption and CO_2 reduction has been studied. Pearce(Pearce, 2009) has studied the various use of CHP and photovoltaic cogeneration networks to increase the application of solar panels. This study showed that the combined use of PV/CHP can not only reduce energy consumption but can increase the use of PV systems in these systems up to five times. Uzunoglu et al. (Uzunoglu et al., 2009)have studied the combination of PV, FC and ultra-capacitor (UC). The purpose of this study was to combine different energy sources to supply the energy required by the fuel cell. Sharma et al.(Sharma & Chandel, 2013) examined the

performance of a 190 kWp photovoltaic power plant. The average annual performance ratio, capacity factor and efficiency of the system are 74%, 9.27% and 8.3%, respectively.

The widespread use of fossil fuels has caused irreparable damage to the world's ecosystem, so one of the concerns facing human societies is finding ways to convert different fuels into usable energy so that there is minimal pollution in the environment. In general, there are two direct and indirect methods for converting fuel into usable energy. In the indirect method, the chemical energy of the fuel is converted into mechanical work and then into electrical energy. Perhaps the first indirect energy converter could be introduced as primary steam engines that did not have the desired efficiency, and then by the invention of internal combustion engines by ironing, this efficiency gradually improved, and with the advancement of thermodynamics, the Carnot cycle, which is the most ideal thermal cycle, has been proposed that the thermal efficiency of the Carnot cycle is limited to the temperature of the two heat sources in which the cycle operates. In the indirect method, due to the combustion at high temperatures, toxic gases such as NO_x and CO are formed, which pollute the environment. In the direct method, the chemical energy of the fuel is directly converted into electrical energy without intermediation. One of the direct energy converters is the fuel cell. A fuel cell is an electrochemical converter consisting of a cathode, an anode, and an electrolyte that converts the chemical energy of the fuel into electrical energy without causing environmental and noise pollution by electrochemical reactions. Unlike a heat engine, a fuel cell does not follow the Carnot cycle and its efficiency is not limited to the Carnot cycle. Hydrogen is a common fuel used in fuel cells, known as a clean fuel, which is mass-produced using renewable sources and the water electrolysis method with the least amount of pollution. The electricity current output from the fuel cell is a direct current (DC) with low voltage, which makes it possible to use the fuel cell in many electrical devices and to produce the required power of each device, the fuel cells can be connected in series which is called a stack (Meratizaman et al., 2015). The history of the fuel cell back to the early nineteenth century, when William Grove was researching the process of electrolysis of water. His experiments in 1839 led to the idea that water electrolysis could be reversed and that electricity could be generated from the chemical reaction of hydrogen and oxygen (Larminie et al., 2003). Each fuel cell consists of three components: anode, cathode, and membrane or electrolyte. Fuel cells are classified from different perspectives. These categories are based on the type of fuel and used oxidizer, fuel conversion site (external or internal), operating temperature, type of ions exchanged and type of electrolyte. The common classification is based on the type of the used electrolyte. Accordingly, fuel cells are divided into 6 categories.

- Polymer membrane fuel cell (PEMFC)
- Phosphoric acid fuel cell (PAFC)
- Alkaline fuel cell (AFC)
- Molten carbonate fuel cell (MCFC)
- Solid oxide fuel cell (SOFC)
- Direct-Methanol fuel cell (DMFC)

Each fuel cell operates at its own temperature, among which, the polymer fuel cell has a short start-up time due to its low operating temperature. Also, different fuels can be used in each fuel cell depending on the type of electrolyte, ion exchanger, and operating temperature, but proportional to the type of fuel cell, some impurities in the fuel can cause fuel cell poisoning. Fuel cells can be used in various industries, such as solid oxide and molten carbonate fuel cells are very useful in power plants, since their membranes are capable of working at high temperatures and can also generate a lot of power. However, in polymer membrane fuel cell, due to the solid and flexible polymer membrane, low temperature, low pollution, and low start-up time, it is a suitable choice for movable applications and portable devices such as UAVs(O'hayre et al., 2016). Bernardi and Verbrugge(Bernardi & Verbrugge, 1991)modeled a portion of the polymer fuel cell, including the electrode and catalyst of the cathode and membrane, as a single-phase, isothermal, one-dimensional, and steady-state. In this modeling, water management, oxygen penetration in the electrode, and calculation of losses in the catalyst, the cathode, and membrane electrodes are considered. This modeling is performed assuming the catalyst is homogeneous the membrane is hydrated, and the gas pressure changes at the electrode are ignored. One of the important results of the modeling is that at a current density of 0.2 A/cm^2 and above, membrane resistance has a significant effect and at a high current density, the reaction speed is increased and the reactant species do not have the opportunity to penetrate most of the cathode catalyst layer and part of the catalyst remains unused. Rowe and Li(Rowe & Li, 2001) proposed a one-dimensional model for a single-phase, non-isothermal polymer fuel cell in steady-state conditions. In this model, the temperature distribution, the effect of generated heat in catalyst, the effects of temperature on the distribution of oxygen concentration, the effect of moisture of the incoming gas on the water molar flux as well as membrane water content, and the effect of water evaporation in the electrode layer are investigated. The assumptions considered in this model are that the amount of pressure and water content of the membrane in the membrane layer changes linearly and the structure of the catalysts and electrodes are homogeneous. The results of this modeling show that by decreasing the water content of the membrane, ohmic losses increase, and with increasing current density, the

temperature gradient in the membrane layer increases, and de-humidification of gases alone cannot prevent the membrane from drying. Ju et al. (Ju et al., 2005)have proposed a single-phase, non-isothermal model for a polymer fuel cell so that pure hydrogen enters the fuel cell as a fuel. In this research, a model for calculating the mechanisms of heat production sources due to activation losses, the electrochemical reaction in the cathode catalyst, and ionic resistance of the membrane is presented and the effect of thermal conductivity of the model shows that the negative effects of heat production in high current density is much more critical at low thermal conductivity and the thermal conductivity of the electrode has a significant effect on the membrane temperature, so the issue of water and heat management is important. In the medium current density range, in cases where the relative humidity is low, due to the increase in membrane temperature, the performance of the fuel cell is significantly reduced, and to improve the performance of the fuel cell, it is necessary to control the performance of the cell by humidifying the inlet gases. Mishra et al. (Mishra et al., 2005)have presented a non-isothermal and one-dimensional model in polymer fuel cells and have studied the effect of various operational parameters of polymer fuel cells including pressure, temperature, humidity, and type of fuel. Also, the optimal state of the geometric parameters of the polymer fuel cell components has been investigated. The optimization is based on the maximum power density (maximum current density at constant voltage) and the optimal value of the parameters of the inlet gas temperature, relative humidity, platinum density and membrane thickness are calculated.

Due to the fact that one of the major problems in the world today is the emission of pollutants from fossil fuels, hydrogen has always been considered a clean fuel. Due to its unique properties, hydrogen is an ideal energy carrier (Veziro & Barbir, 1992). The benefits of hydrogen include:

- At relatively high efficiencies, hydrogen can be generated from electricity or converted to it.
- It can be stored in gaseous form (suitable for large-scale storage), in liquid form (suitable for air and space transportation), or the form of metal hydrides (suitable for land vehicles and other relatively small storage equipment).
- It can be transported by pipeline or by tankers over long distances.
- It can be converted into other forms of energy in more efficient ways than any other fuel (such as catalytic combustion, electrochemical conversion, etc.) (Mahishi et al., 2014).

Hydrogen production is an important step in replacing hydrogen with fossil fuels. By performing various processes on many primary energy sources such as fossil fuels (coal, crude oil, natural gas, etc.), nuclear fuels (such as thorium, thorium, uranium, etc.), geothermal energy as well as solar, wind and tidal energy can produce hydrogen. These energy sources are divided into two categories: renewable and non-renewable. The major technologies for hydrogen production are fossil fuels, biomass, and water. Hydrogen is generated from fossil fuels by steam reforming from natural gas, thermal fission of natural gas, partial oxidation (POX) or coal gasification; From biomass by incineration, fermentation, pyrolysis, gasification and then liquefaction or biological production; It is produced from water by electrolysis, photolysis, thermochemical processes, thermolysis and a combination of biological, thermal and electrolytic processes (Godula-Jopek, 2015). The most logical source of large-scale hydrogen production is water. Methods of hydrogen production from water include electrolysis, direct thermal decomposition or thermolysis, thermochemical processes, and photolysis. Among all methods of hydrogen production, water decomposition is considered due to its high efficiency, non-pollution production, hydrogen production, and pure oxygen. Hydrogen generation by water electrolysis is a developed technology that is based on a simple and highly efficient method that is appropriate for large-scale hydrogen production due to its efficiency in the range of 72% -82% (Gupta, 2008). Electrolyzer technology is divided into four general categories: alkaline electrolyzers whose electrolyte is liquid (for example, KOH), proton exchange membrane electrolyzers (PEM), anion exchange membrane electrolyzers (AEM), which both have solid polymer electrolytes, and solid oxide electrolyzers that use ceramic membranes (Bessarabov et al., 2016). Using a simple electrochemical model, Ni et al. (Ni et al., 2008)analyzed the polarization curve of a polymer membrane electrolyzer to produce hydrogen. The effect of temperature on polarization curve and electrolyzer performance has been investigated in this study. In another study (Ni et al., 2006), the polymer membrane electrolyzer system in combination with a system that supplies some of its input energy from renewable energy sources such as the solar thermal energy to heat the incoming water, has been investigated and energy and exergy analysis has been performed on this system.

In the current study, a power supply system required for the drone is developed according to Figure 1 so that its main fuel, hydrogen, is stored in a storage tank. PEM fuel cell uses this fuel to supply the required power of the drone. Water is the output of PEM according to its electrochemical reaction. By using a photovoltaic system and solar radiation, the energy required by the PEM electrolyzer can be provided to convert the water produced by the PEM fuel cell into hydrogen and oxygen. Applying this method recovers part of the drone's consumable hydrogen and oxygen. As a result, the fuel runs out later and will lead to more flight continuity. The following describes the relationships of different

parts of the system.

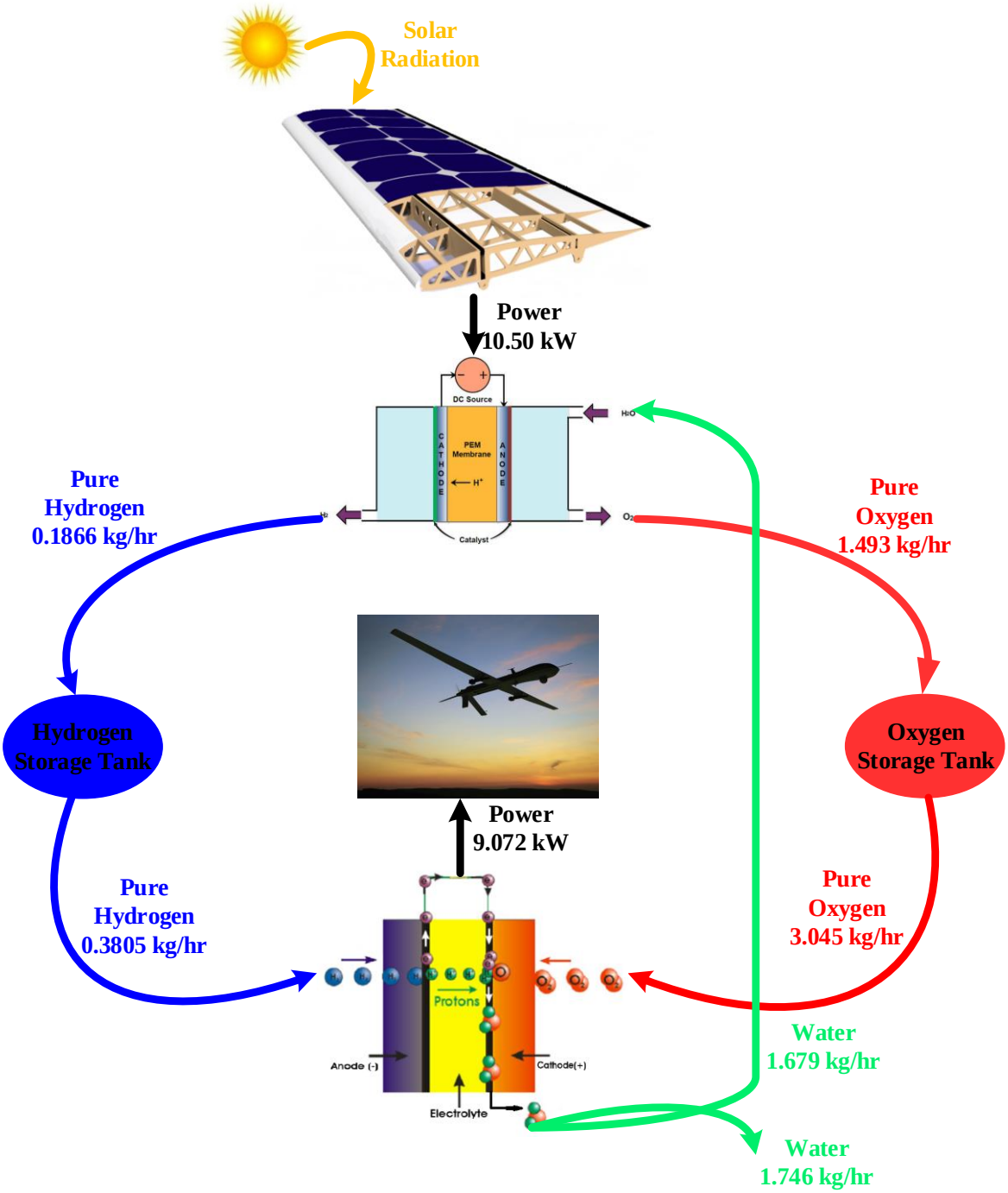

Figure 1 Block flow diagram of the proposed system

2. Material and methods

The main components of the proposed system are a photovoltaic panel, PEM fuel cell, and PEM electrolyzer, each of which is described separately in this section. In the following, the thermodynamic relationships governing each of these components are discussed.

2.1. Photovoltaic panel

As mentioned in the present study, the required energy supply is provided by an embedded hydrogen tank. Using solar energy through a photovoltaic panel, the required energy of the electrolyzer can be generated in order to produce more hydrogen in addition to stored hydrogen. Photovoltaic cells are made of several thin layers of silicon, which release electrons inside the cell when exposed to sunlight. By absorbing radiation, the electrons of the silicon atom are deflected, leaving positive holes. Free electrons and holes are next to each other in the normal state. Therefore, electrons and holes must be separated to generate electricity. This is done by

injecting opposite charges into the cell layers. As a result, electrons cannot return to the positive charge of the holes. When an external electrical connection is made, free electrons flow in the circuit towards the positive charge holes, which causes an electric current. To evaluate the performance of photovoltaic systems, several performance parameters were provided by the International Energy Agency (IEA) (Besheer et al., 2019; Li et al., 2017; Sharma & Chandel, 2013). These parameters include Reference Yield, Array Yield, Final System Yield, Array capture losses, System's total energy loss, and so on. In the following, the relevant relations are given in Figure 2 (equations 1-5) (Ghorbani et al., 2021).

In addition, the system performance ratio can be defined as the deduction of the final system yield to the reference yYield(Ghorbani et al., 2020).

$$PR = Y_F / Y_R \quad (6)$$

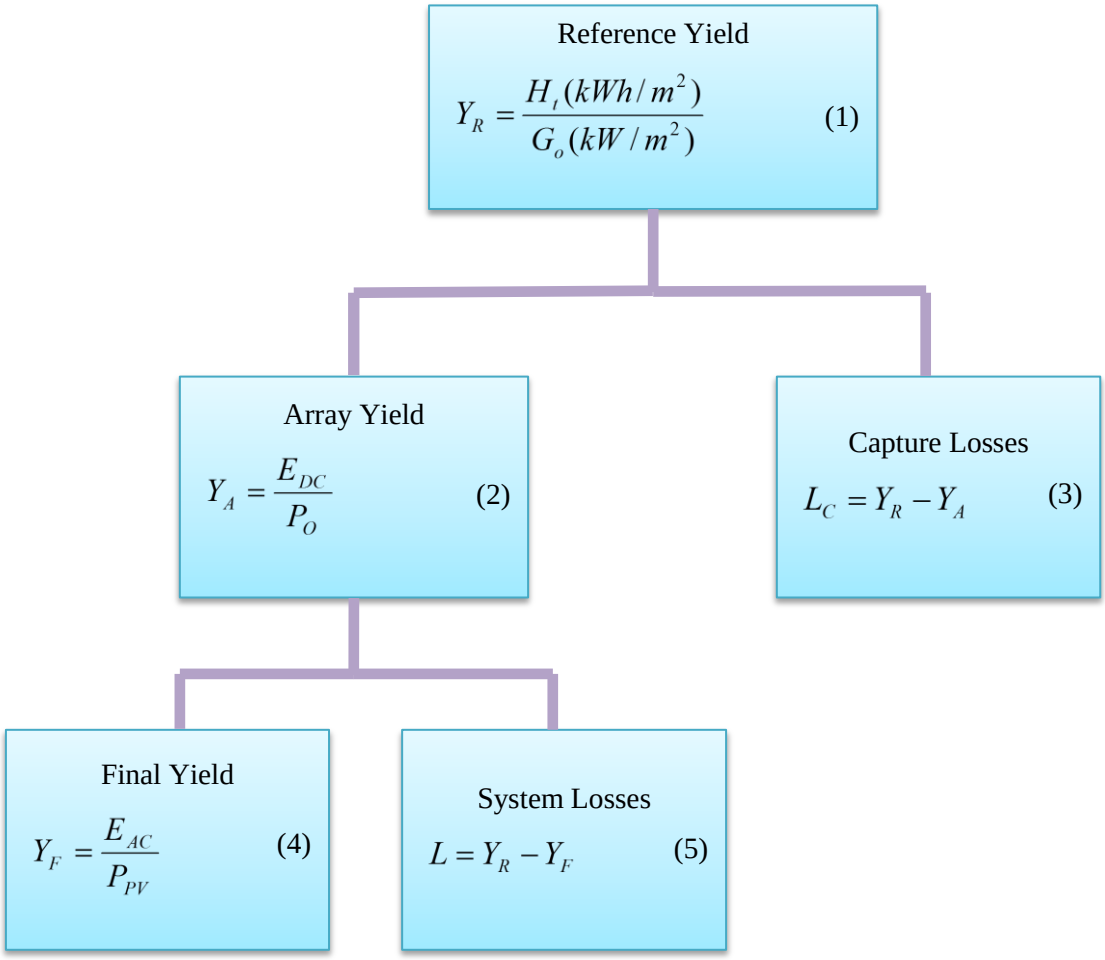

Figure 2 Flowchart of PV system performance

2.2. PEM fuel cell

As mentioned, the fuel cell converts fuel and oxidant energy directly into electrical energy. The maximum electrical potential that a fuel cell can be achieved when it operates under reversible conditions. Equation 7 represents the first law of thermodynamics. The work can be divided into two parts: electrical work and work due to expansion, which is in the form of Equation 8, and in thermodynamic relations, the relationship of work due to expansion is written as Equation 9(O'hayre et al., 2016).

$$d\hat{u} = \delta q - \delta w \quad (7)$$

$$\delta w = \delta w_p + \delta w_e \quad (8)$$

$$\delta w_p = Pdv \quad (9)$$

For a reversible system, the second law of thermodynamics is written as the following equation.

$$ds = \frac{\delta q}{T} \quad (10)$$

By combining relations 7 to 10, the relationship of electrical work with thermodynamic parameters is established.

$$d\hat{u} = Tds - Pdv - \delta w_e \quad (11)$$

For the relationship between electrical work and Gibbs free energy of reaction, Gibbs free energy relations have been used and by merging

equations 11 to 13, the relation of electrical work with temperature, pressure, and Gibbs energy is obtained as Equation 14 (O'hayre et al., 2016).

$$h = \hat{u} + Pv \longrightarrow dh = d\hat{u} + Pdv + v \quad (12)$$

$$g = h - Ts \longrightarrow dg = dh - Tds - sdT \quad (13)$$

$$dg = -\delta w_e + vdP - sdT \quad (14)$$

The fuel cell in the open circuit mode can be considered as isothermal and isobar and equation 14 is simplified as the following equation finally, the relationship between electrical work and Gibbs free energy is obtained.

$$dg = -\delta w_e \quad (15)$$

The reversible voltage of a fuel cell can be calculated using the relationship between electrical work and Gibbs free energy and the number of moles of produced electrons per mole of fuel, and its value depends on the temperature, pressure, and concentration of species entering the fuel cell because Gibbs free energy reaction is dependent on these quantities, so the amount of Gibbs free energy is calculated under standard conditions. The definition of electrical work is as follows: $E°_r$ is the reversible voltage of the fuel cell under standard conditions and Q is the amount of electrical charge created by consuming one mole of fuel (O'hayre et al., 2016).

$$w_e = E_r^0 \times Q \quad (16)$$

Using the number of moles of produced electrons in the oxidation reaction of the anode region and also with the help of the Faraday number which expresses the number of electrical charges in one mole of electrons, the amount of electric charge created by the chemical reaction of the fuel cell can be calculated.

$$Q = n \times F \quad (17)$$

Using the relation of electrical work with Gibbs free energy and equations 16 and 17, the amount of reversible voltage can be obtained in standard conditions as the following equation (O'hayre et al., 2016).

$$E_r^0 = -\frac{\Delta g^0}{nF} \quad (18)$$

The reversible voltage of the fuel cell is a function of the temperature, pressure, and concentration of the species participating in the reaction. In general, the amount of reversible voltage can be calculated from the Nernst equation (Ebrahimi et al., 2022).

$$E_r = E_T - \frac{RT}{nF}\ln\frac{\prod_{product}^{vi} a}{\prod_{reactant}^{vi} a} \quad (19)$$

In Equation 19, E_T represents the effect of temperature on the reversible voltage and the second expression represents the effect of pressure and concentration on the reversible voltage of the fuel cell. Parameter a indicates the activity of the species, which for ideal gases is defined as the ratio of partial pressure to gas pressure. Table 1 shows the activity of ideal solids, liquids, and gases, but the water vapor pressure cannot exceed the saturation pressure, so the water vapor activity can be calculated as follows.

$$a_{vapor} = \frac{P_i}{P_{sat}} \quad (20)$$

The relationship between the effect of temperature on the reversible voltage of the fuel cell under standard conditions is given in the following equation. According to the equation, the higher the temperature of the fuel cell, the lower the amount of reversible voltage.

$$E_T = E_r^0 - \frac{\Delta s}{nF}(T - T_0) \quad (21)$$

Due to losses, the reversible potential decreases with increasing current. These losses originate from three main sources, which are activation, resistance, and concentration losses. Therefore, to analyze the fuel cell, a performance curve is used that shows the voltage in terms of current. It should be noted that the output current from the cell depends on the active level of the fuel cell, so instead of the current, a quantity called the current density, which is equal to the ratio of current to the surface of the fuel cell is used to compare fuel cells of different sizes with each other (Ebrahimi et al., 2022). When hydrogen and oxygen molecules penetrate the surface of the catalyst, a certain amount of energy is required to perform the reaction, which is called activation energy. To supply this energy, a portion of fuel cell voltage must be used for this operation and cause electrochemical reactions to occur, resulting in a voltage drop across the anode and cathode catalysts, which is called the activation drop. The amount of activation loss is almost independent of the current density. The reaction of hydrogen oxidation in the anode catalyst produces electrons and protons, and these charged species must reach the cathode catalyst to perform the reduction reaction. The membrane conduct proton and the electrodes and the external circuit conduct the electrons, and there is a resistance to the transfer of charged species into the components of the polymer fuel cell, which decreases the voltage and is expressed as the resistance (ohmic) drop. Resistance loss increases linearly with increasing current density. Voltage drop due to species concentration is usually caused by high current density. When a large current is taken from the fuel cell, the rate of reactions at the catalyst site increases, and the required reactant species must pass through the electrode porous medium at high speed and reach the reaction site, However, when the reacting species pass through the porous medium, its pressure and concentration drop, so the concentration of the species in the catalyst decreases sharply, and the polymer fuel

cell experiences a sharp drop in voltage at high current density. In the special case where the species transfer rate and the species reaction rate in the catalysts are equal so that there is no accumulation of species in the catalyst, a limit current density is created and the fuel cell current density cannot exceed this value. To obtain the output voltage of the fuel cell, we must first obtain the reversible voltage and calculate the output voltage of the fuel cell by reducing the expressed losses (Ebrahimi et al., 2022).

$$V = E_r - (\eta_{act} + \eta_{ohm} + \eta_{conc}) \quad (22)$$

Figure 3 shows the performance curve of a polymer fuel cell in which the triple loss zones of the polymer fuel cell voltage are shown(Larminie et al., 2003).

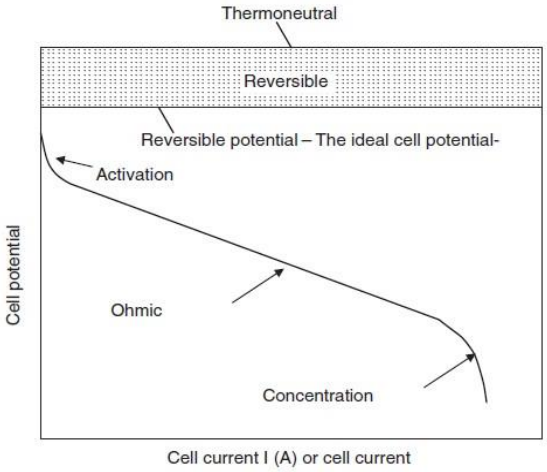

Figure 3 Polymer fuel cell performance curve (Larminie et al., 2003)

2.3. PEM electrolyzer

Water electrolysis is a process in which water is electrochemically decomposed into hydrogen and oxygen molecules according to the following reaction.

$$H_2 + \frac{1}{2}O_2 + Electricity \longrightarrow H_2O \quad (23)$$

Polymer membrane electrolyzer is considered because of their several advantages such as high current density, high voltage efficiency, fast system response, wide current density range which is equivalent to more flexible production speed, the possibility of higher pressure difference across the membrane, compact design system, the possibility of combining electrolyzer and fuel cell, high purity of gas and ability to combine with other renewable energy systems such as solar, wind, etc. (Ni et al., 2008). In polymer membrane electrolyzers, a polymer electrolyte membrane (proton exchange membrane) is used for ion conduction. According to the following reactions, water is oxidized on the anode side to produce oxygen, and hydrogen is produced on the cathode side.

$$H_2O(L) \longrightarrow \frac{1}{2}O_2(g) + 2H^+ + 2e^- \text{ anode side} \quad (24)$$

$$2H^+ + 2e^- \longrightarrow H_2(g)\ cathode\ side \quad (25)$$

The electrolyte of a polymer membrane electrolyzer is a thin ion-conducting solid membrane instead of the aqueous solution used in an alkaline electrolyzer. The membrane carries the H^+ ion (proton) from the anode to the cathode, separating the hydrogen and oxygen gases. The most commonly used membrane is nafion. The main advantage of the polymer membrane electrolyzer over other electrolyzers is that the polymer membrane electrolyzer is safer and more reliable due to the lack of corrosive electrolytes. In addition, the ability to operate at high-pressure differences on both sides of the membrane prevents oxygen compression. This is especially important when the electrolyzer is operating under oscillating conditions. The single-cell voltage of the electrolyzer is defined as follows(Kianfard et al., 2018).

$$V = V_{oc} + V_{act} + V_{ohm} + V_{con} \quad (26)$$

In the above relation, V_{oc} is open-circuit voltage, V_{act} is an activation voltage drop and V_{Con} is a voltage drop across the anode and cathode (concentration) and V_{ohm} is Ohmic voltage drop. The required relationships to calculate the terms of the above equation are available in the reference (Nami et al., 2017).

3. System validation

The use of PV systems to generate power from solar radiation energy has been validated in several studies. In this paper, MATLAB software is used to model the solar photovoltaic system. The proposed PV model was validated with reference (Khatib & Elmenreich, 2016). A comparison of the results shows that it has good compatibility with the mentioned references with a power of 200 watts. Figure 4 shows the current and power generated by the PV system for different voltages, respectively. Fuel cell and electrolyzer simulation are validated in the present work with reliable sources in the field and are given in Figures 5 and 6, respectively (Ioroi et al., 2002; Ni et al., 2008; Spiegel, 2011). According to these figures, the simulations have proper compatibility with the mentioned research.

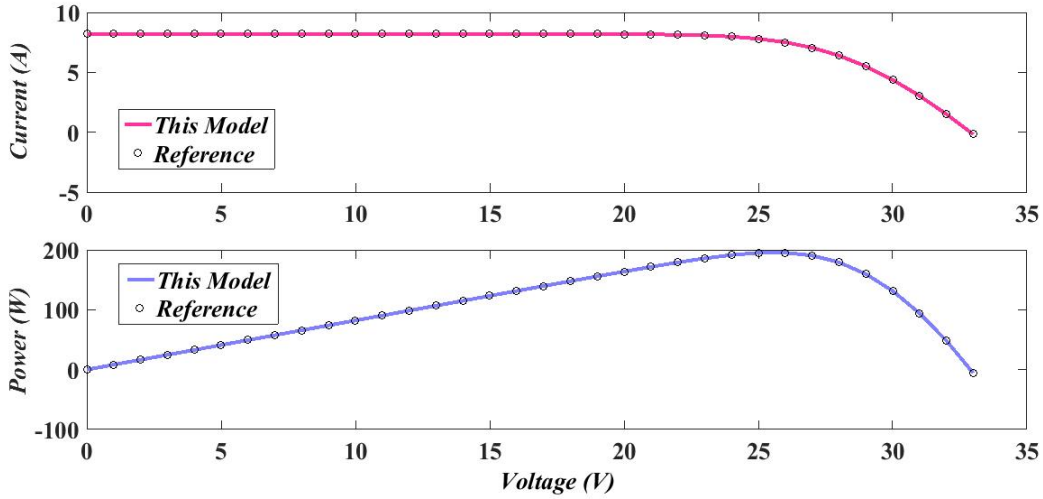

Figure 4 Validation of the PV modeling in this study

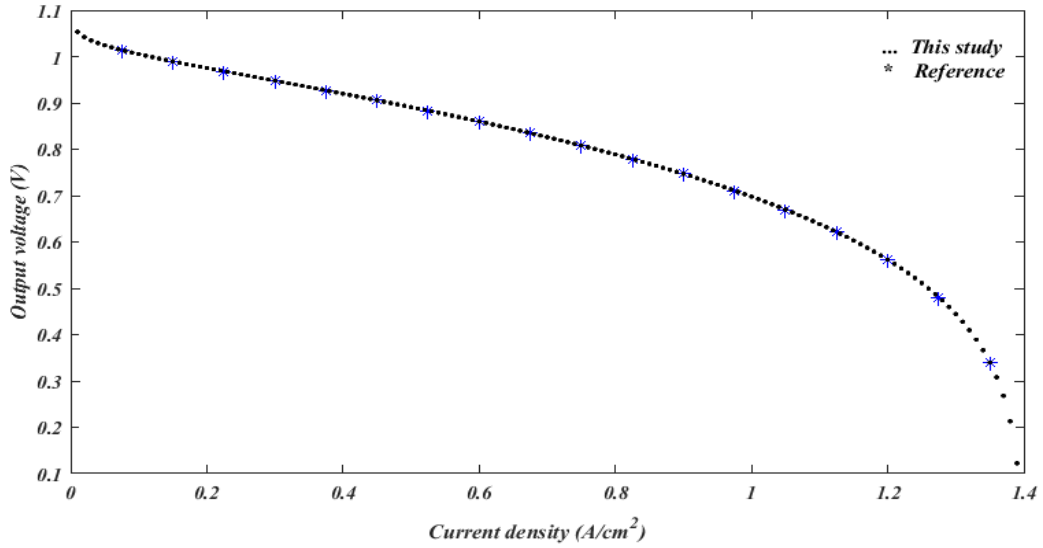

Figure 5 PEM fuel cell validation results

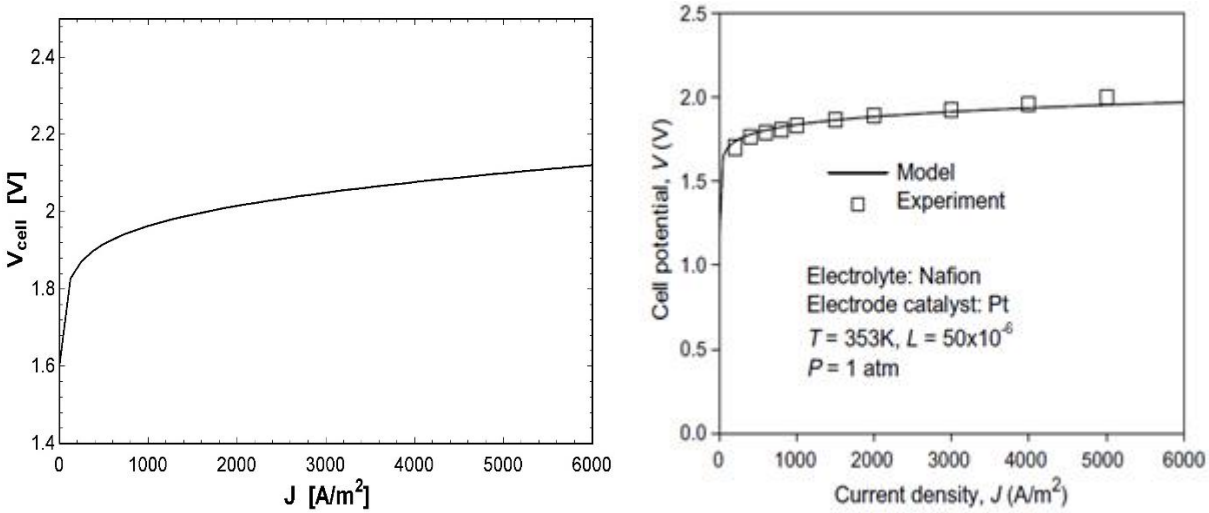

Figure 6 Validation of the PEM electrolyzer modeled in this study

4. Results and discussion

In this section, the results of the proposed system are given. According to Figure 1, in the present study, the purpose is to supply the UAV power through the PEM fuel cell so that part of the required hydrogen and oxygen is provided by the PEM electrolyzer (part by the electrolyzer and the rest by the hydrogen and oxygen storage tanks in the UAV). Some of the UAV's energy is generated by in-flight solar energy using a photovoltaic panel. In this regard, an attempt is made to generate 10 kW of system output power for UAVs (it should be noted that the variety of UAVs used for various purposes leads to generating of a variety of UAVs in terms of weight and dimensions and consequently the capacity of the propulsion system. In the present study, the required propulsion system capacity is assumed to be 10 kW). Exactly 9,072 kW of net power is generated by the PEM fuel cell 0.3805 kg/h of pure hydrogen and 3.045 kg/h of pure oxygen are needed, some of which are produced by a PEM electrolyzer. In the simulated electrolyzer, 0.1866 kg/h of pure hydrogen and 1.493 kg/h of pure oxygen are produced, and in return, 10.50 kW of power is consumed, which must be generated by the photovoltaic panel. The difference between the consumable hydrogen and oxygen of the fuel cell and the hydrogen and oxygen produced by the electrolyzer must be provided by the storage tank built into the drone. The required power of the electrolyzer is 10.50 kW which is supplied by the photovoltaic system. For this, first, a 200 W photovoltaic panel module is simulated. Next, to achieve an output power of 10.50 kW, it is enough to scale up and obtain the required panel level of the modules. Table 2 shows the specifications of the proposed different parts. In the following sections, the results related to the PEM fuel cell and PEM electrolyzer, as well as the PV system, are presented separately.

Table 1 Activity of ideal solids, liquids and gases

activity	phase
solids	$a_i = 1$
liquids	$a_i = 1$
Ideal gas	$a_i = \frac{P_i}{P_0}$

4.1. PV system results

PV system is used to supply the energy required by the system. It is necessary to mention that in the initial simulation, the module temperature is considered to be 25 °C. Also, the amount of solar radiation is considered to be 1000 $^{W}/_{m^2}$and by changing them, the results will be reviewed.

- **The results of changing the module temperature**

In this section, the module temperature is changed from 10 to 40 °C and the results are reported. In Figure 7, the module temperature is assumed to be 10 °C. According to the figure, the maximum output power is obtained at a voltage of 27 V, which is 221.2 W. Also, the maximum output current is at 15 V, which is 8.687 A. Figure 8 shows the simulation at the module temperature of 15 °C. According to the figure, the maximum output power at a voltage of 27 V is 212.2 W, which is reduced by 10 °C compared to the module temperature. Regarding the output current, it can be said that the maximum value is obtained at 15 V, which is 8.528 A. This amount of current is less than the previous state (temperature of 10 °C). Figure 9 shows the power and current output of the simulated photovoltaic system at 20 °C. According to the figure, increasing the temperature of the module is led to a further reduction of power and current output of the PV system, so that at this module

temperature, the maximum output power at a voltage of 26 V is 204 W, and also the maximum electric current at a voltage of 14 V is calculated to be 8.369 A. Figure 10 shows the amount of power and current generated by the simulated photovoltaic system at 25 °C. Based on this figure, increasing the temperature of the module is led to a further reduction of power and current output of the PV system, so that at this module temperature, the maximum output power at a voltage of 26 V is 195.3 W and also the maximum electric current at a voltage of 13 V is calculated to be 8,210 A. Figure 11 shows the simulation at the module temperature of 30 °C. According to this figure, the maximum output power at 25 V is 187.5 W, which is reduced compared to the module temperature of 25 °C. Figures 12 and 13show the power and current output of the simulated photovoltaic system at temperatures of 35 and 40 °C, respectively. According to these figures, increasing the module temperature is led to a further reduction in power and current output of the PV system, so that at module temperatures of 35 and 40 °C, respectively, the maximum output power is reduced to 179.1 and 171.7 W, respectively and also maximum electric current is reduced to 7.892 and 7.733 A.

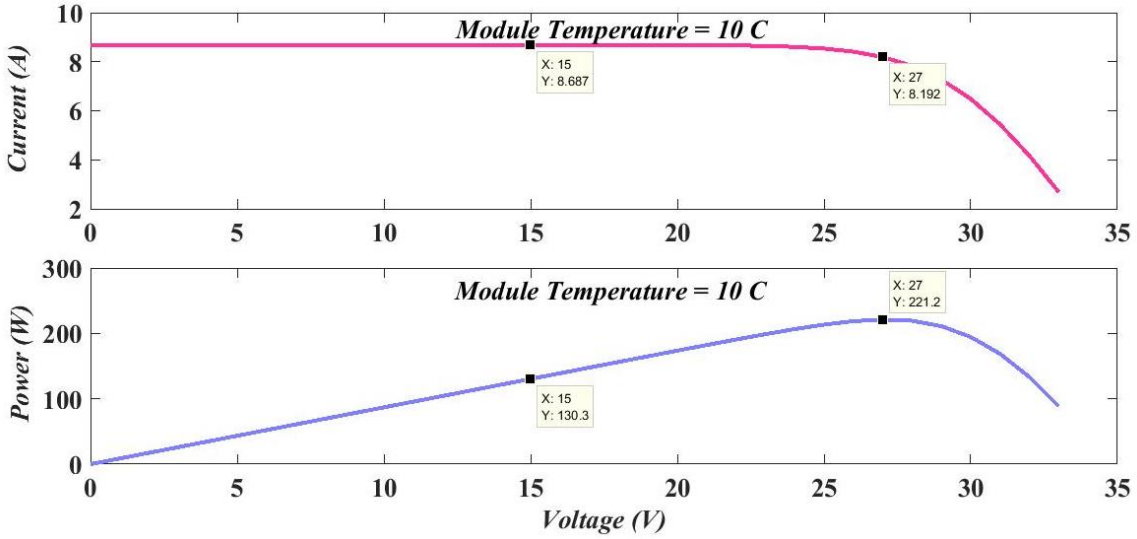

Figure 7 PV system different module temperature (T=10°C)

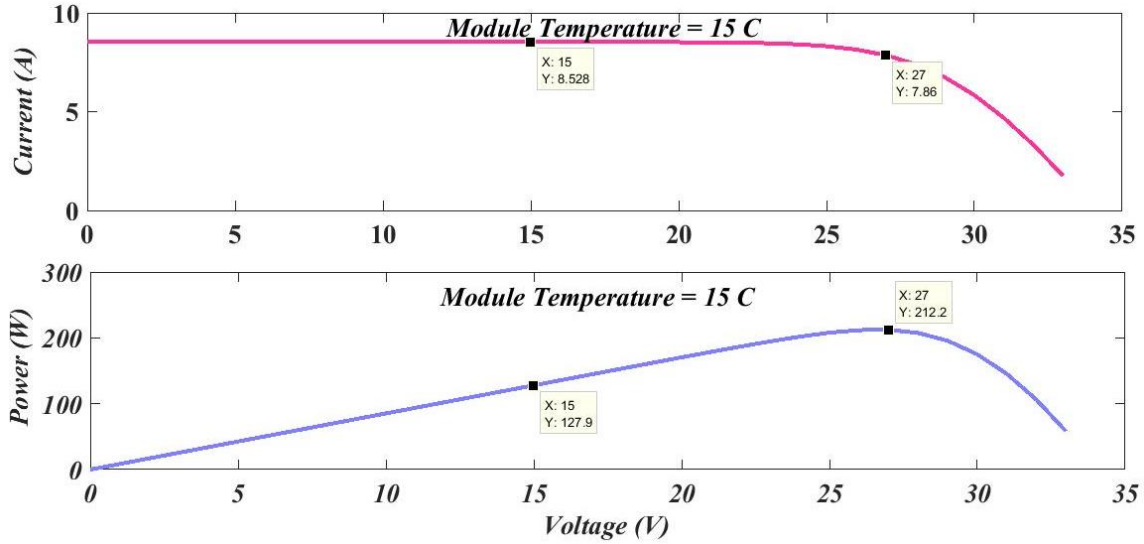

Figure 8 PV system different module temperature (T=15°C)

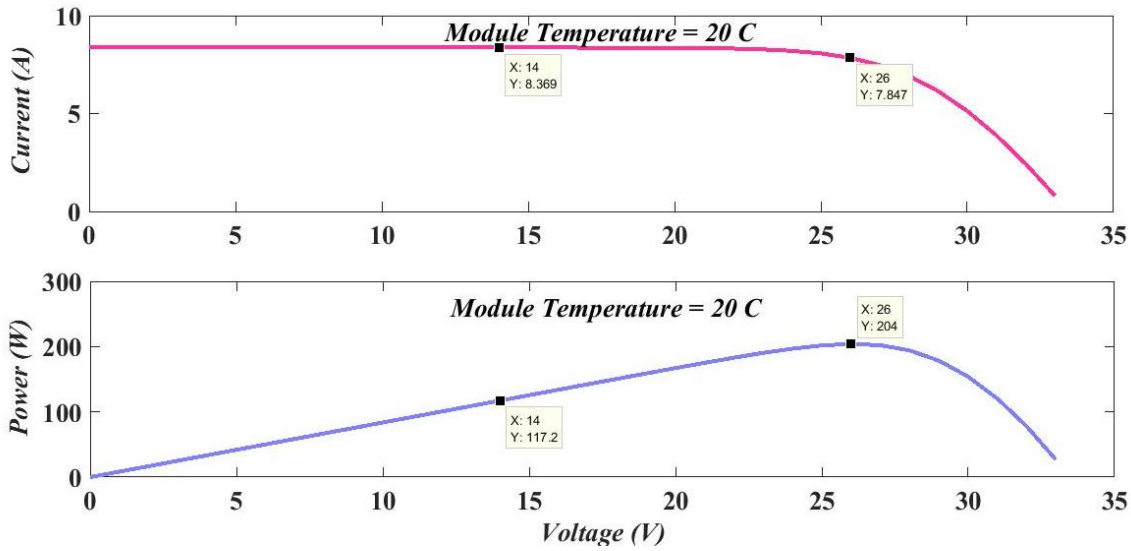

Figure 9 PV system different module temperature (T=20°C)

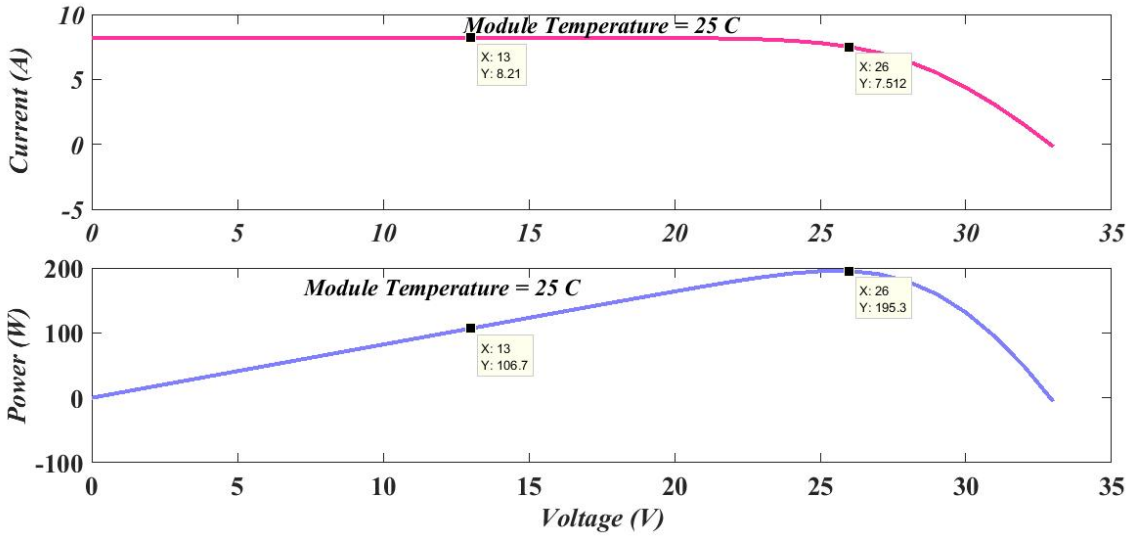

Figure 10 PV system different module temperature (T=25°C)

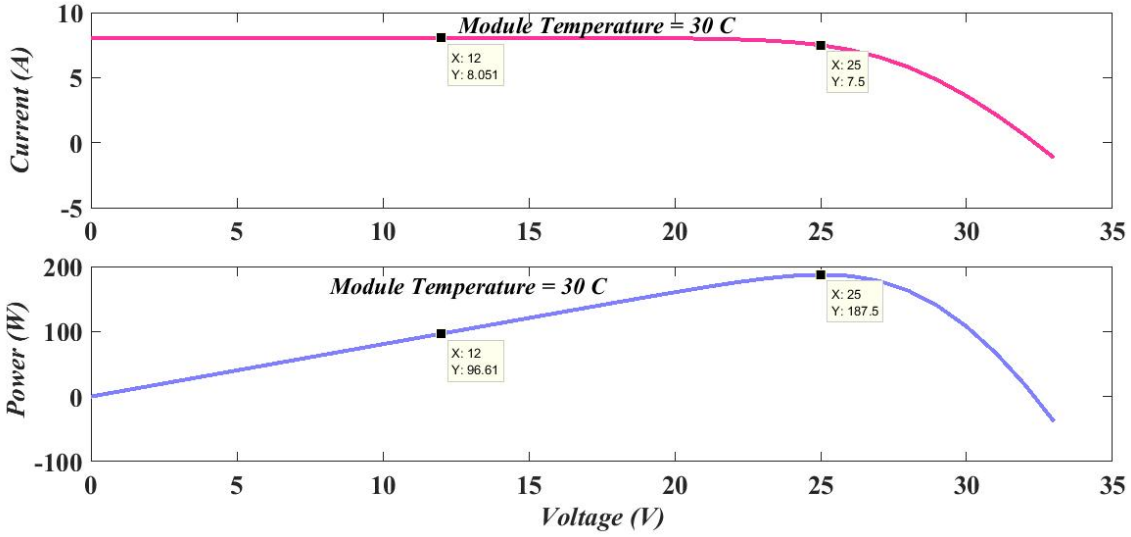

Figure 11 PV system different module temperature (T=30°C)

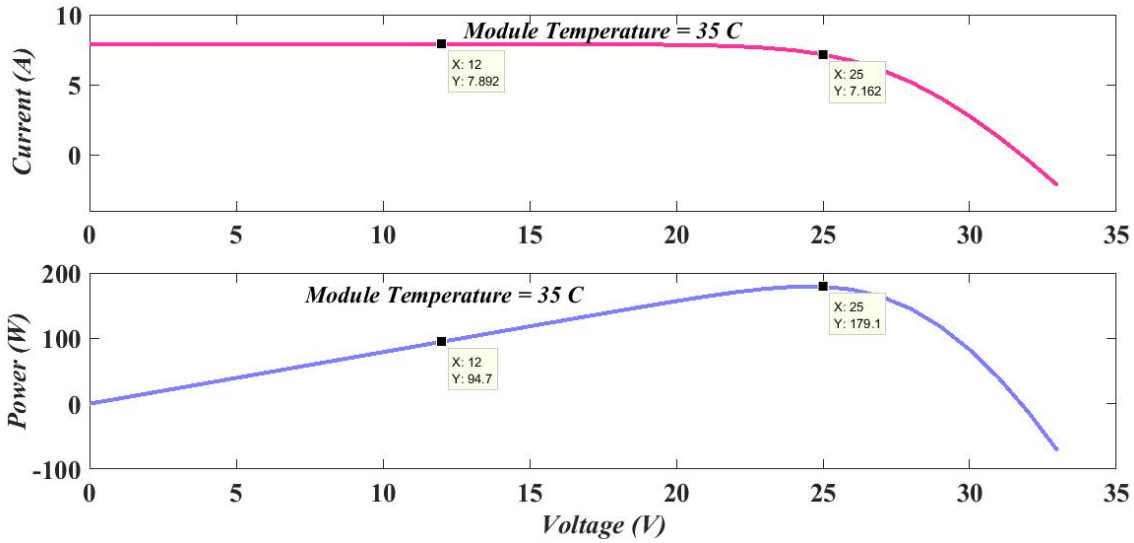

Figure 12 PV system different module temperature (T=35°C)

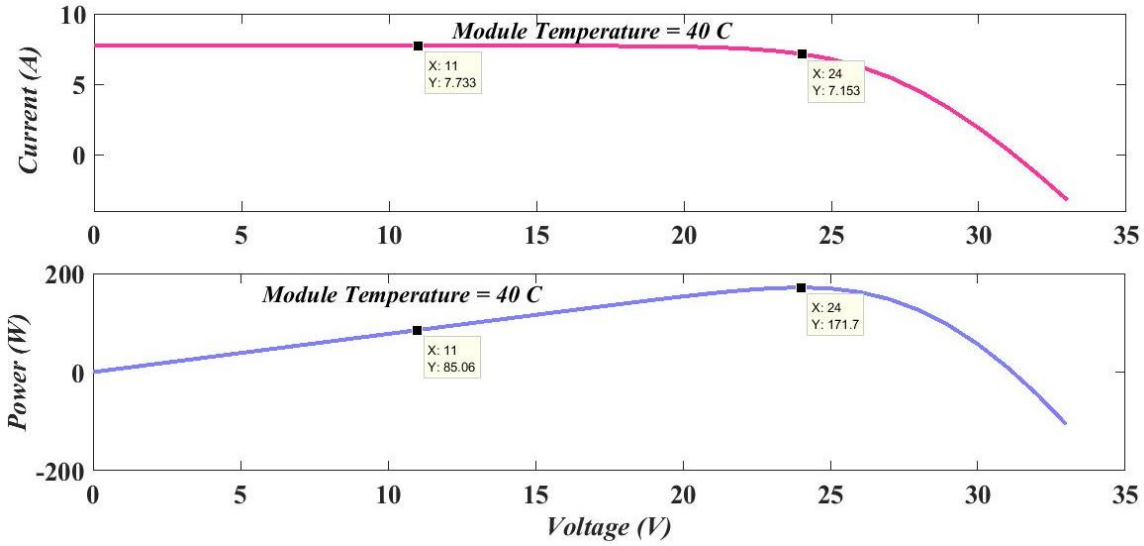

Figure 13 PV system different module temperature (T=40°C)

- **The results of changing the level of solar radiation**

In this section, by changing the level of solar radiation, changes in power and current output of the photovoltaic panel are studied. For this, the solar radiation was changed from 600 $^{W}/_{m^2}$to 1200 $^{W}/_{m^2}$ and the results were reviewed. It should be noted that the temperature of the module in these changes is constant and equal to 25 °C. Figure 14 shows the output current and power of the PV system in 600 $^{W}/_{m^2}$ of solar radiation. Based on the figure, the maximum output power at a voltage of 26 V is 118.7 W. Figure 15shows the results for 700 $^{W}/_{m^2}$ of solar radiation. According to this figure, the maximum output power increases to 138.3 W and also the maximum output current to 5.746 A. Figure 16shows the results for 800 $^{W}/_{m^2}$of solar radiation. According to this figure, there is a further increase in the power and current output of the PV system, so that the maximum power increases to 157.6 W. Figure 17shows the results for radiation at 900 $^{W}/_{m^2}$ As expected, the output power and current increase, and the maximum output power and electric current reach 176.6 W and 7.389 A, respectively. The results for solar radiation of 1000 $^{W}/_{m^2}$ are shown in Figure 18, which is obtained at a module temperature of 25 °C. In Figures 19 and 20, the results for solar radiation of 1100 and 1200 $^{W}/_{m^2}$ are reported. According to these figures, by increasing solar radiation, the generated power, and electric current increase so that in solar radiation of 1100 and 1200 $^{W}/_{m^2}$, the output power of the PV system increases to 213.7 and 232.1, respectively. Also, the generated electric current increases to 9,031 and 9,852 A, respectively.

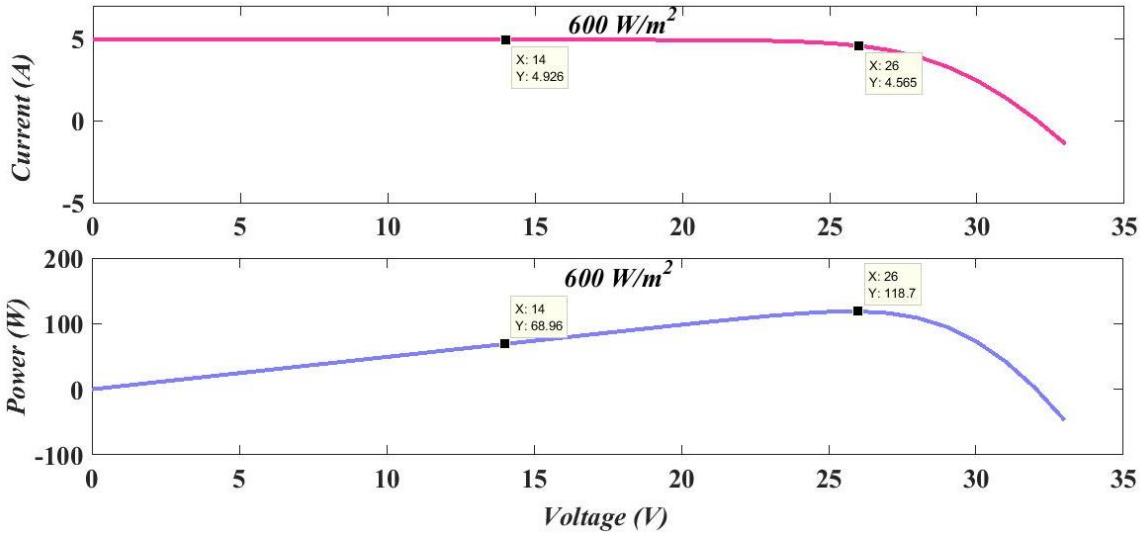

Figure 14 PV system different solar radiation (600 W/m2)

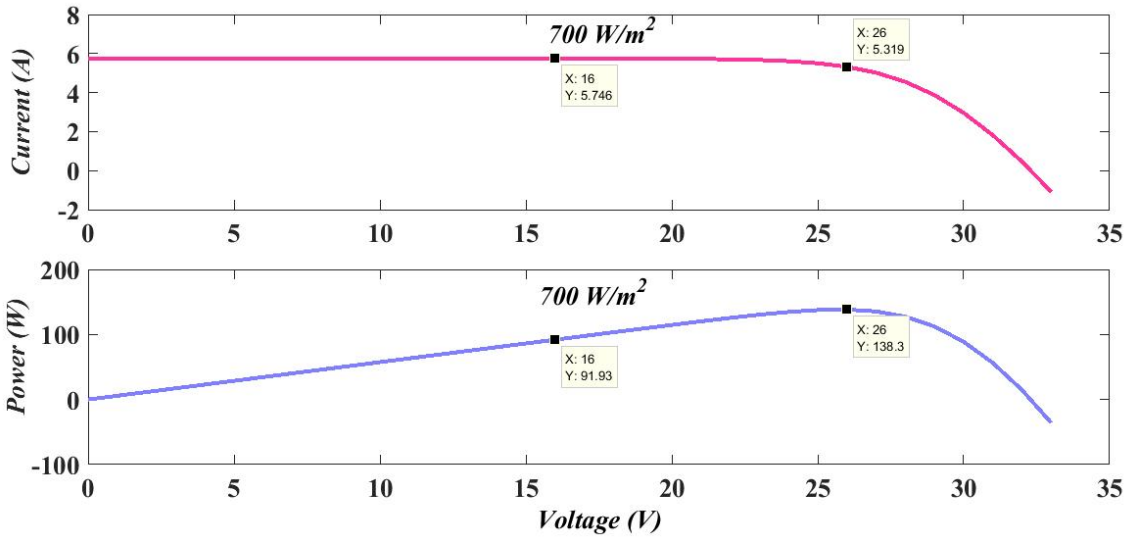

Figure 15 PV system different solar radiation (700 W/m2)

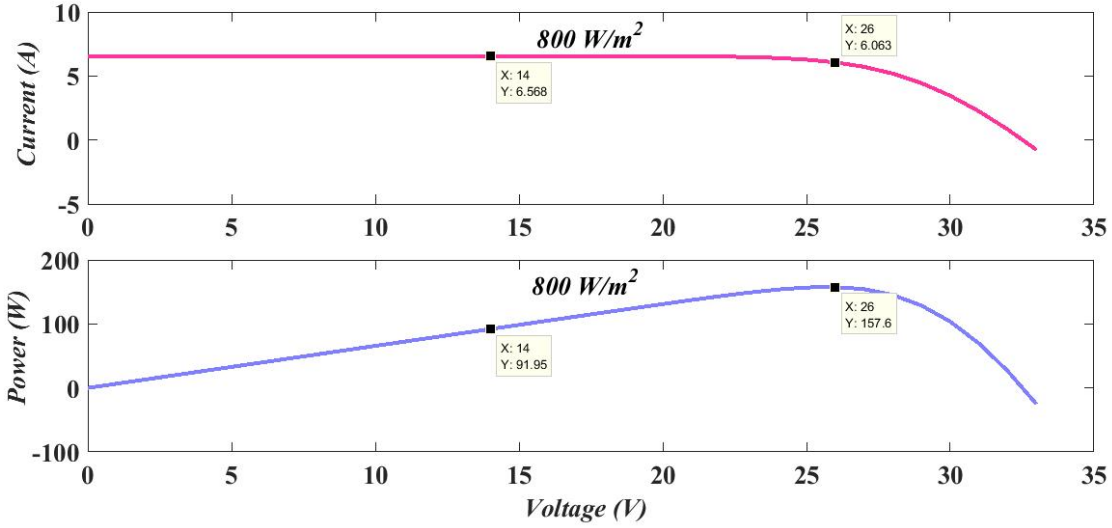

Figure 16 PV system different solar radiation (800 W/m2)

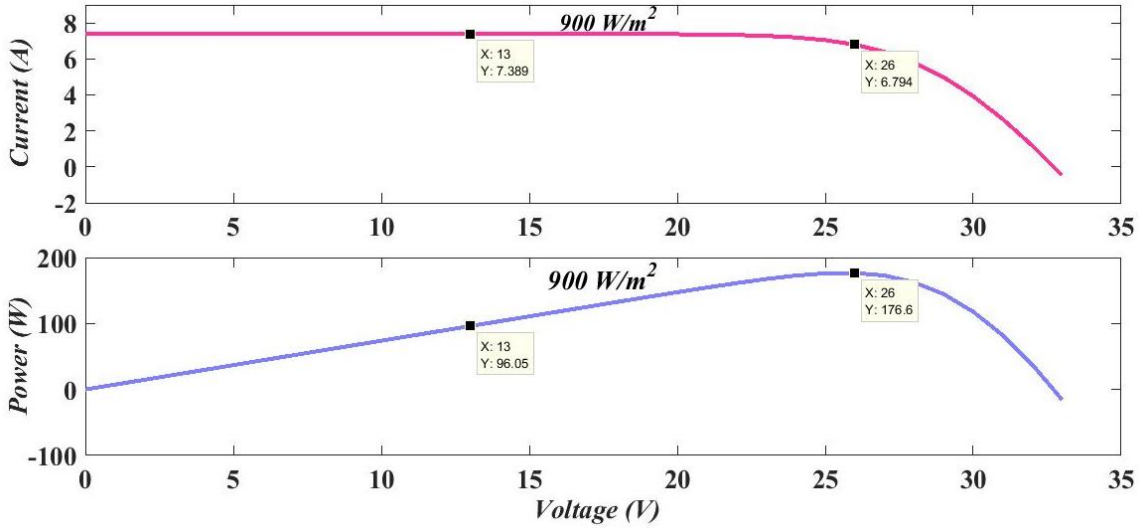

Figure 17 PV system different solar radiation (900 W/m2)

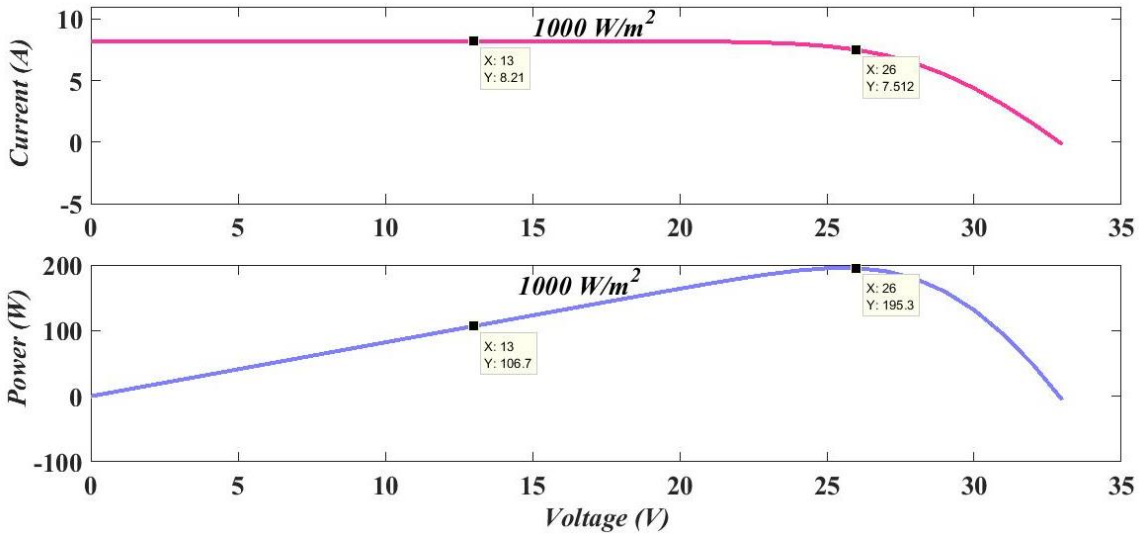

Figure 18 PV system different solar radiation (1000 W/m2)

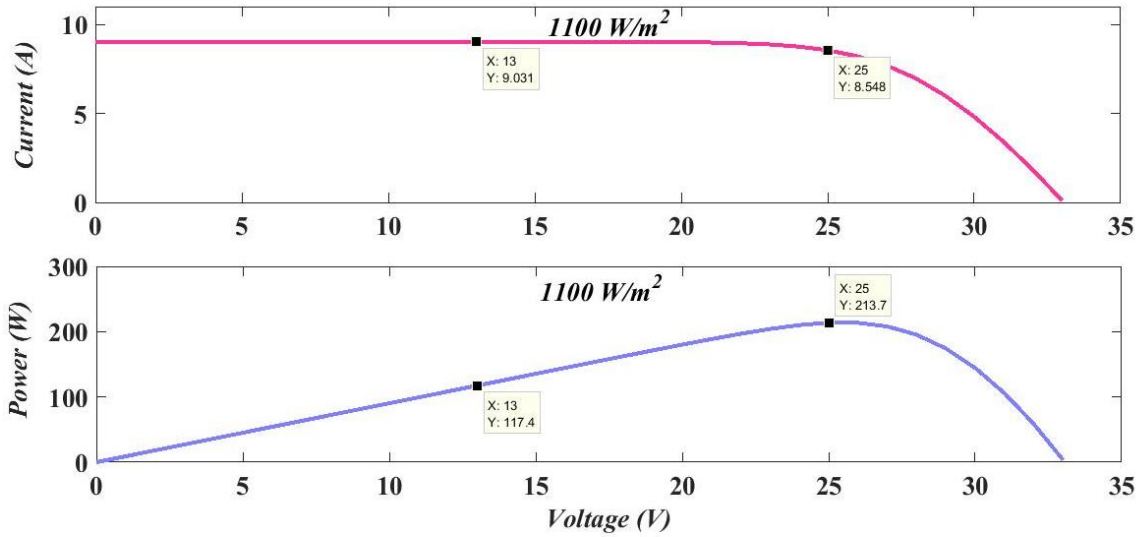

Figure 19 PV system different solar radiation (1100 W/m2)

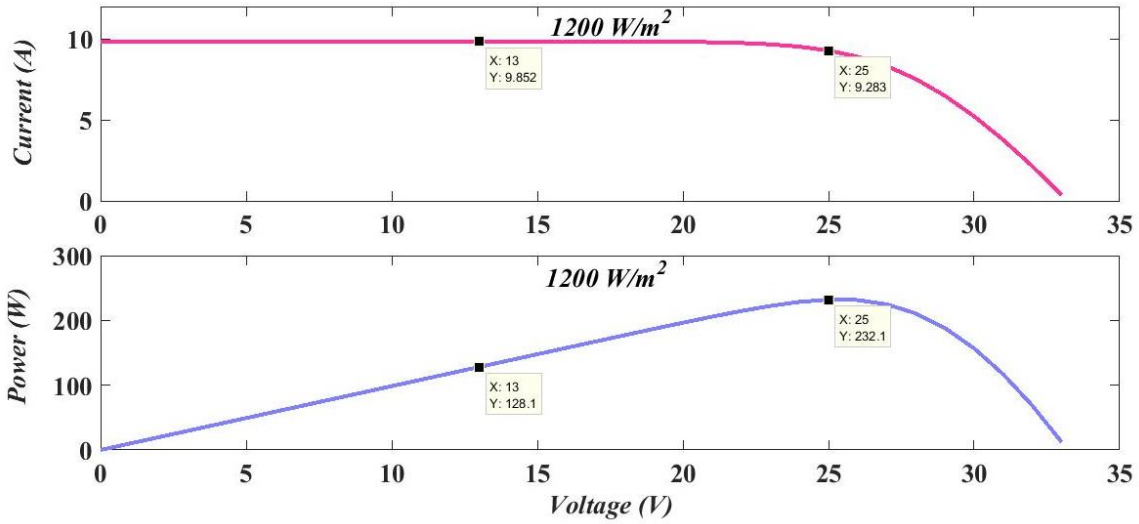

Figure 20 PV system different solar radiation (1200 W/m2)

4.2. The Results of PEM fuel cell

In the present study, the power supply mechanism required for UAV propulsion is a PEM fuel cell. One of the most important parameters of a fuel cell is its current density. Then, by changing this parameter, its effect on other fuel cell outputs is reported.

Figure 21shows the amount of consumable hydrogen and oxygen as well as the amount of water generated by the cell for different amounts of current density. As the current density increases, the consumption of hydrogen and oxygen in the cell, as well as the generated water, naturally increases. Figure 22shows the activation, concentration, and ohmic overpotential fuel cell at different current densities. As the current density increases, the all voltage drops decrease. In contrast, the ideal output voltage of the fuel cell (Nernst voltage), as well as the useful output voltage of the fuel cell for different current densities, are shown in Figure 23. According to this figure, by increasing current density, the Nernst voltage as well as the useful voltage of the cell decreases.

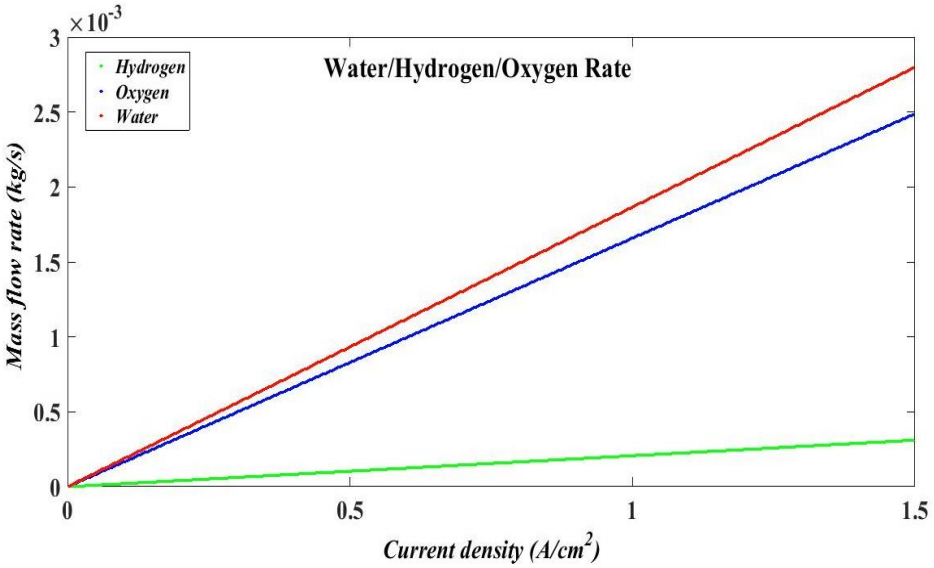

Figure 21 PEM fuel cell results at different current density (Water/Hydrogen/Oxygen rate)

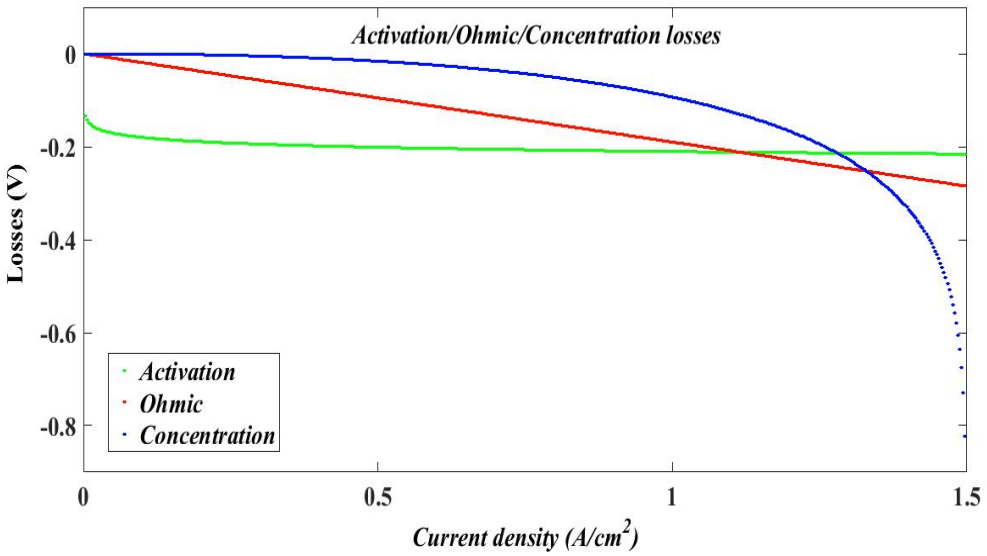

Figure 22 PEM fuel cell results at different current density (Activation/Ohmic/Concentration losses)

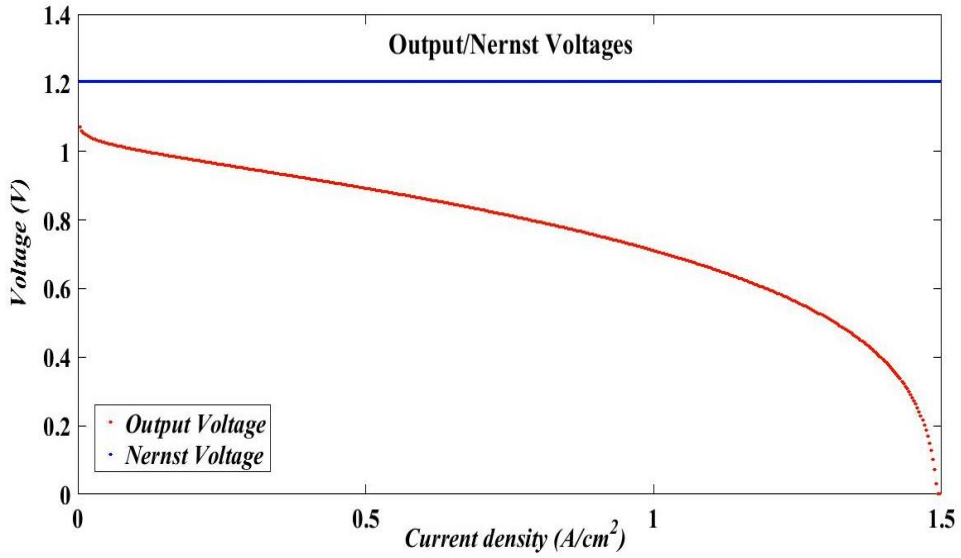

Figure 23 PEM fuel cell results at different current density (Output voltage vs. Nernst voltage)

4.3. The results of PEM electrolyzer

According to the results, the electrolyzer simulated in the present study consumes 10.50 kW of power, and in contrast, generates 0.1866 kg/h of pure hydrogen and 1.493 kg/h of pure oxygen. The amounts of hydrogen and oxygen generated by the electrolyzer as well as its water consumption in different current densities are shown in Figure 24. The power consumption of the electrolyzer at different current densities is shown in Figure 25. Based on this figure, by increasing current density, its power consumption also increases. It should be noted that in the basic condition, at a current density of 5000 $^{A}/_{cm^2}$(0.5 $^{A}/_{m^2}$), the power consumption of the electrolyzer is 10.50 kW. Figure 26 displayes the changes in electrolyzer energy efficiency at different current densities. According to this figure, by increasing current density, the energy efficiency of the electrolyzer decreases exponentially. The energy efficiency of the electrolyzer at a current density of 5000 $^{A}/_{m^2}$is 59.92%.

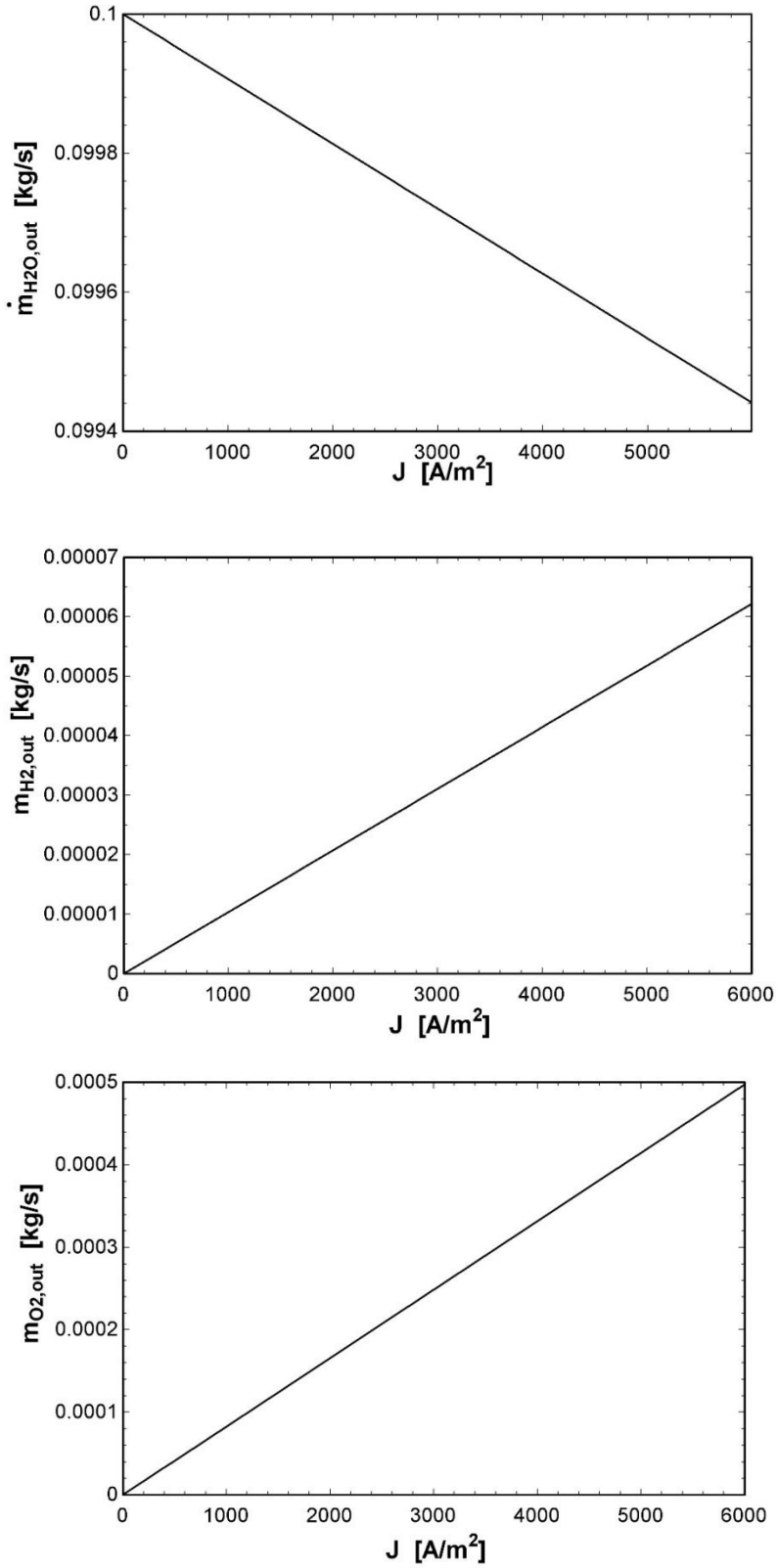

Figure 24 PEM electrolyzer results at different current density (Water/Hydrogen/Oxygen rate)

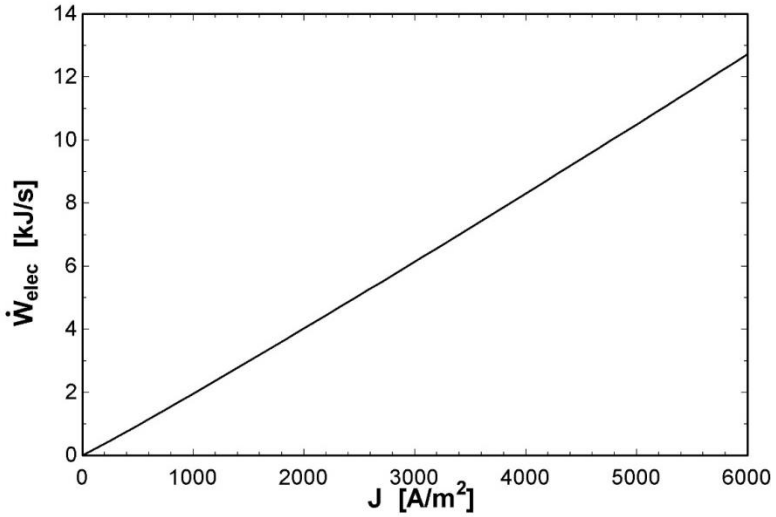

Figure 25 PEM electrolyzer results at different current density (power consumption)

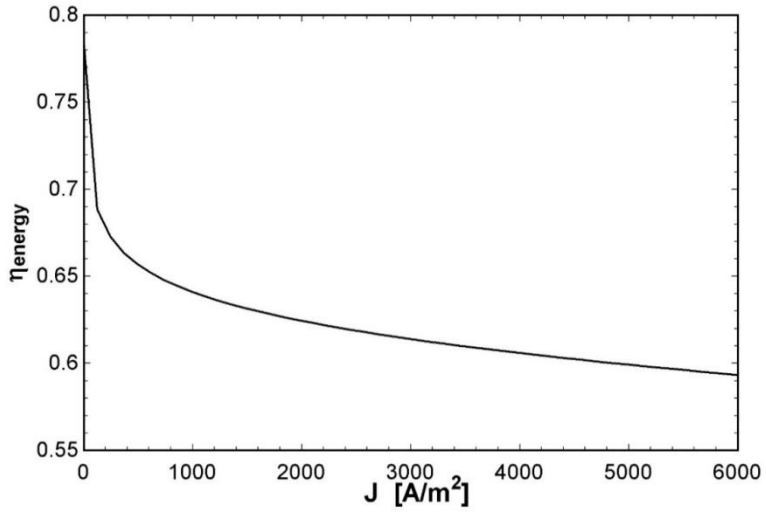

Figure 26 PEM electrolyzer results at different current density (energy efficiency)

5. Conclusion

In the current study, a modern power generation system for UAVs consisting of PEM electrolyzer, PEM fuel cell, photovoltaic panel, and hydrogen and oxygen storage tanks is developed. Initially, the fuel cell and PEM electrolyzer sections were modeled, so that to generate 9,072 kW of power by the PEM fuel cell, 3,805 kg/h of pure hydrogen and 3,045 kg/h of pure oxygen are required, part of which is generated by the PEM electrolyzer. In the simulated electrolyzer, 0.1866 kg/h of pure hydrogen and 1.493 kg/h of pure oxygen are produced, and in return, it consumes 10.50 kW of power, which must be produced by photovoltaic panels. The difference between the consumable hydrogen and oxygen of the fuel cell and the hydrogen and oxygen generated by the electrolyzer must be supplied by their storage tank. By changing the current density of the PEM electrolyzer and PEM fuel cell, the performance of these two parts was evaluated. It was stated that by enhancing current density, the energy efficiency of the fuel cell decreases. In the basic cycle, at a current density of 0.51 $^{A}/_{cm^2}$, the energy efficiency of the fuel cell is 70.93%. The energy efficiency of the fuel cell for current densities greater than 1 $^{A}/_{cm^2}$ is less than 60%. Increasing the current density affects the output power of the PEM fuel cell so by enhancing the current density to 1.11 $^{A}/_{cm^2}$, the cell output power raises and reaches a maximum of 14.51 kW, but with a further increase in current density, the output power of the fuel cell is reduced. As the current density increments, the energy efficiency of the electrolyzer decreases exponentially. The energy efficiency of the electrolyzer at a current density of 5000 $^{A}/_{m^2}$ is 59.92%. In the following, the simulation of the photovoltaic panel was put on the agenda to complete the propulsion system developed in this study. By changing the module temperature and solar radiation level, the performance of the PV system was evaluated. By decreasing the

temperature of the module and also increasing the level of solar radiation, the output capacity of the PV system increases so that at temperatures below 20 °C or solar radiation more than 1000 W/m, the output capacity of the PV system reaches more than 200 W. In general, it can be concluded that the proposed system is feasible as a propulsion system for UAVs with different capacities. The main advantage of the proposed system is the increase in the flight continuity of UAVs through the use of solar renewable energy, which as an auxiliary system, regenerates part of the consumable hydrogen and oxygen of the UAV. This depletes the UAV fuel over long distances.

Nomenclature

ΔG	Gibbs free energy change, (kJ mol^{-1})
ΔH	enthalpy change, (kJ mol^{-1})
ΔS	entropy change, (kJ mol^{-1} K^{-1})
A	Area
E	thermodynamic voltage (v)
J	current
j	current density
F	Faraday's constant
R_a	anode resistance
R_c	cathode resistance
R_{tot}	internal resistance of fuel cell
V	Voltage
G_O	Array Reference Irradiance (kW/m2)
Ex	Exergy
H_t	Total in-plane Solar Radiation (kWh/m2)
h	Enthalpy
L_C	Capture losses
L	System losses
$\dot{m}$	Mass flow rate (kg/s)
P	Pressure
P_{PV}	PV Array Maximum Power (kW)
Q	Volumetric flow rate
R	Universal gas constant (8.314 J/ mol. K)
r	Ohmic Resistance (Ωm^2)
T	Temperature
U	Thermal Loss Factor ($kW/m^2.K$)
s	Entropy
$\dot{W}$	Work rate
Y_F	Final Yield (kWh/kWp/day)
Y_R	Reference Yield ($kWh/m^2.day$)
Y_A	Array Yield (kWh/kWp/day)

Greek letters

η	Efficiency, (%)
υ	kinematic viscosity of the ambient air, (m^2/s)
β	volumetric expansion coefficient of the ambient air/k
σ	Stephen Boltzmann constant, (5.6705×10^{-8} $Wm^{-2}K^{-4}$)
α	Absorbance of the PV modules

Abbreviations

AEM	Anion exchange membrane
AFC	Alkaline fuel cell
CHP	Cogeneration heat and power
DC	Direct current
DMFC	Direct-Methanol fuel cell
FC	Fuel cell
IEA	International energy agency
MCFC	Molten carbonate fuel cell
PAFC	Phosphoric acid fuel cell
PEM	Polymer exchange membrane
POX	Partial oxidation
PV	Photovoltaic
SOFC	Solid oxide fuel cell
UAV	Unmanned aerial vehicle
UC	Ultra-capacitor

References

Z. Pan, L. An, and C. Wen, "Recent advances in fuel cells based propulsion systems for unmanned aerial vehicles," *Applied Energy,* Vol. 240, pp. 473-485, 2019.

A. Gong and D. Verstraete, "Fuel cell propulsion in small fixed-wing unmanned aerial vehicles: Current status and research needs," *International journal of hydrogen energy,* Vol. 42, No. 33, pp. 21311-21333, 2017.

M. N. Boukoberine, Z. Zhou, and M. Benbouzid, "A critical review on unmanned aerial vehicles power supply and energy management: Solutions, strategies, and prospects," *Applied Energy,* Vol. 255, p. 113823, 2019.

T. Adão *et al.*, "Hyperspectral imaging: A review on UAV-based sensors, data processing and applications for agriculture and forestry," *Remote Sensing,* Vol. 9, No. 11, p. 1110, 2017.

M. Gadalla and S. Zafar, "Analysis of a hydrogen fuel cell-PV power system for small UAV," *International Journal of Hydrogen Energy,* Vol. 41, No. 15, pp. 6422-6432, 2016.

Z. U. Bayrak, U. Kaya, and E. Oksuztepe, "Investigation of PEMFC performance for cruising hybrid powered fixed-wing electric UAV in different temperatures," *International Journal of Hydrogen Energy,* Vol. 45, No. 11, pp. 7036-7045, 2020.

B. Ghorbani, A. Ebrahimi, M. Moradi, and M. Ziabasharhagh, "Continuous production of cryogenic energy at low-temperature using two-stage ejector cooling system, Kalina power cycle, cold energy storage unit, and photovoltaic system," *Energy Conversion Management,* Vol. 227, p. 113541, 2021.

D. A. R. Pandey, Reji & Mahendran, S.. (2022). Solar energy: direct and indirect methods to harvest usable energy. 10.1016/B978-0-12-818206-2.00007-4. .

F. N. Muhammad Asif Hanif, Rida Tariq, Umer Rashid,, *Renewable and Alternative Energy Resources*. Academic Press, 2022.

Z. A. Smith and K. D. Taylor, *Renewable and alternative energy resources: a reference handbook*. ABC-CLIO, 2008.

P. Degobert, S. Kreuawan, and X. Guillaud, "Micro-grid powered by photovoltaic and micro turbine," in *International Conference on*

Renewable Energies in France, 2006.
M. Medrano, A. Castell, G. Fontanals, C. Castellón, and L. F. Cabeza, "Economics and climate change emissions analysis of a bioclimatic institutional building with trigeneration and solar support," *Applied Thermal Engineering,* Vol. 28, No. 17-18, pp. 2227-2235, 2008.
J. M. Pearce, "Expanding photovoltaic penetration with residential distributed generation from hybrid solar photovoltaic and combined heat and power systems," *Energy,* Vol. 34, No. 11, pp. 1947-1954, 2009.
M. Uzunoglu, O. Onar, and M. Alam, "Modeling, control and simulation of a PV/FC/UC based hybrid power generation system for stand-alone applications," *Renewable energy,* Vol. 34, No. 3, pp. 509-520, 2009.
V. Sharma and S. Chandel, "Performance analysis of a 190 kWp grid interactive solar photovoltaic power plant in India," *Energy,* Vol. 55, pp. 476-485, 2013.
M. Meratizaman, S. Monadizadeh, A. Ebrahimi, H. Akbarpour, and M. Amidpour, "Scenario analysis of gasification process application in electrical energy-freshwater generation from heavy fuel oil, thermodynamic, economic and environmental assessment," *international journal of hydrogen energy,* Vol. 40, No. 6, pp. 2578-2600, 2015.
J. Larminie, A. Dicks, and M. S. McDonald, *Fuel cell systems explained*. J. Wiley Chichester, UK, 2003.
R. O'hayre, S.-W. Cha, W. Colella, and F. B. Prinz, *Fuel cell fundamentals*. John Wiley & Sons, 2016.
D. M. Bernardi and M. W. Verbrugge, "Mathematical model of a gas diffusion electrode bonded to a polymer electrolyte," *AIChE journal,* Vol. 37, No. 8, pp. 1151-1163, 1991.
A. Rowe and X. Li, "Mathematical modeling of proton exchange membrane fuel cells," *Journal of power sources,* Vol. 102, No. 1-2, pp. 82-96, 2001.
H. Ju, H. Meng, and C.-Y. Wang, "A single-phase, non-isothermal model for PEM fuel cells," *International Journal of Heat Mass Transfer,* Vol. 48, No. 7, pp. 1303-1315, 2005.
V. Mishra, F. Yang, and R. Pitchumani, "Analysis and design of PEM fuel cells," *Journal of power sources,* Vol. 141, No. 1, pp. 47-64, 2005.
T. Veziro and F. Barbir, "Hydrogen: the wonder fuel," *International Journal of Hydrogen Energy,* Vol. 17, No. 6, pp. 391-404, 1992.
M. Mahishi *et al.*, "'Hydrogen production from biomass and fossil fuels," ed: Boca Raton, FL, USA: CRC Press, 2014, pp. 113-137.
A. Godula-Jopek, *Hydrogen production: by electrolysis*. John Wiley & Sons, 2015.
R. B. Gupta, *Hydrogen fuel: production, transport, and storage*. Crc Press, 2008.
D. Bessarabov, H. Wang, H. Li, and N. Zhao, *PEM electrolysis for hydrogen production: principles and applications*. CRC press, 2016.
M. Ni, M. K. Leung, and D. Y. Leung, "Energy and exergy analysis of hydrogen production by a proton exchange membrane (PEM) electrolyzer plant," *Energy conversion management,* Vol. 49, No. 10, pp. 2748-2756, 2008.
M. Ni, M. K. Leung, and D. Y. Leung, "Electrochemistry modeling of proton exchange membrane (PEM) water electrolysis for hydrogen production," *Proceeding of the WHEC,* Vol. 16, 2006.
C. Li *et al.*, "Performance of off-grid residential solar photovoltaic power systems using five solar tracking modes in Kunming, China," *International Journal of Hydrogen Energy,* Vol. 42, No. 10, pp. 6502-6510, 2017.
A. H. Besheer, M. A. Eldreny, H. M. Emara, and A. Bahgat, "Photovoltaic energy system performance investigation: case study of 5.1-kW rooftop grid tie in Egypt," *Journal of Energy Engineering,* Vol. 145, No. 3, p. 05019001, 2019.
B. Ghorbani, A. Ebrahimi, M. Moradi, and M. Ziabasharhagh, "Energy, exergy and sensitivity analyses of a novel hybrid structure for generation of Bio-Liquefied natural Gas, desalinated water and power using solar photovoltaic and geothermal source," *Energy Conversion Management,* vol. 222, p. 113215, 2020.
A. Ebrahimi, B. Ghorbani, M. Delpisheh, and M. H. Ahmadi, "A comprehensive evaluation of a novel integrated system consisting of hydrogen boil-off gas reliquifying process and polymer exchange membrane fuel cell using exergoeconomic and Markov analyses," *Energy Reports,* Vol. 8, pp. 1283-1297, 2022.
H. Kianfard, S. Khalilarya, and S. Jafarmadar, "Exergy and exergoeconomic evaluation of hydrogen and distilled water production via combination of PEM electrolyzer, RO desalination unit and geothermal driven dual fluid ORC," *Energy conversion management,* Vol. 177, pp. 339-349, 2018.
H. Nami, E. Akrami, and F. Ranjbar, "Hydrogen production using the waste heat of Benchmark pressurized Molten carbonate fuel cell system via combination of organic Rankine cycle and proton exchange membrane (PEM) electrolysis," *Applied Thermal Engineering,* Vol. 114, pp. 631-638, 2017.
T. Khatib and W. Elmenreich, *Modeling of photovoltaic systems using Matlab: Simplified green codes*. John Wiley & Sons, 2016.
C. Spiegel, *PEM fuel cell modeling and simulation using MATLAB*. Elsevier, 2011.
T. Ioroi, K. Yasuda, Z. Siroma, N. Fujiwara, and Y. Miyazaki, "Thin film electrocatalyst layer for unitized regenerative polymer electrolyte fuel cells," *Journal of Power sources,* Vol. 112, No. 2, pp. 583-587, 2002.